

1 Writing abstracts

Usually the abstract for a talk or a paper gives a brief summary or preview of the work you've accomplished. Someone can scan through the abstract and then see whether they should attend your talk or read your paper, according to their interests. Then, it is important to highlight your work in an appropriate way so your intended audience is attracted to your work! This means that you should keep in mind to include some relevant *keywords* that will lead an internet search to your work. The keywords are the important terms or phrases that are very specific to your topic.

The abstract should include the following:

- Describe the problem or topic of interest (system, materials, model, etc.)
- State what are the new advances or results, and relate to other work.
- State how the results were obtained (experimental or computational method, etc.).

These don't have to be in this order, but they should be included somewhere.

As far as the length, if you look at many articles, you will see the length can range from one sentence on up to many paragraphs. Usually, however, a single short paragraph is good. You can really include these three points, without much elaboration, which is left for the actual talk or manuscript.

In the case of an abstract for a talk, which may be published in some conference proceedings, more details about the results can be included in the abstract. Furthermore, in some cases it may be useful also to include a diagram or graph of results.

Writing style varies considerably, especially depending on the journal, from very technical or dry to much more elegant or intriguing. Compare the examples included here.

A unified model for the long and high jump

O. Helene^{a)}

Instituto de Física, Universidade de São Paulo, C.P. 66318, CEP 05315-970 São Paulo, SP, Brasil

M. T. Yamashita

Unidade Diferenciada de Itapeva, Universidade Estadual Paulista, CEP 18409-010 Itapeva, SP, Brasil

(Received 4 February 2005; accepted 26 June 2005)

A simple model based on the maximum energy that an athlete can produce in a small time interval is used to describe the high and long jump. Conservation of angular momentum is used to explain why an athlete should run horizontally to perform a vertical jump. Our results agree with world records. © 2005 American Association of Physics Teachers.
[DOI: 10.1119/1.2000975]

I. INTRODUCTION

A few years ago, William Harris asked how the kinetic energy acquired from running is converted in the long and high jump events.¹ The question was whether athletes running horizontally can change their velocity into one that forms an angle of 45° with the horizontal without changing their speed. The three negative answers²⁻⁴ were that athletes cannot convert their initial horizontal velocity into a vertical one,³ because it is impossible to generate the necessary power required by the task,⁴ or equivalently, athletes cannot sustain the necessary acceleration to acquire the vertical velocity at takeoff.²

If the answer were positive, the center of mass of a world class athlete running at 10 m/s and taking off at 45° would go a horizontal distance of about 10.2 m. Because the athlete's center of mass is forward of the front edge of the runway at takeoff and behind the point where her heels hit the ground at landing (see Sec. III), the actual total jump length would be about 11 m. For the high jump, the athlete's center of mass would attain a maximum height of 3.5 m. These results are much greater than actual records. We conclude that athletes cannot totally change their horizontal velocity into a vertical one, as stated by the negative answers.

The negative answers bring some new questions. If the magnitude of the velocity is assumed to be unchanged and thus the kinetic energy, why is extra power necessary? Why does a high jumper run horizontally to jump vertically? How do runners change their horizontal velocity into a velocity with a vertical component? What is conserved and what is changed at takeoff?

II. WHAT LIMITS AN ATHLETE'S PERFORMANCE?

There are three systems that any animal uses to produce energy.⁵ For humans and activities whose duration is longer than a few minutes, aerobic energy is produced at a low rate by burning carbohydrates or fats. For activities that last a few tens of seconds, the main source of energy is the breakdown of glycogen in the absence of oxygen and the production of lactic acid. For very short duration activities the body uses the adenosine triphosphate (ATP) stored in muscles, and energy is supplied immediately, following the conversion of ATP into adenosine diphosphate (ADP).

The static force generated from muscle contraction can be very high. However the magnitude of the force is limited by the rate that the muscles can produce energy, which is limited by the rate that ATP is depleted (ATP depletion is com-

pleted in a few seconds). For example, after a few seconds sprinters no longer accelerate, but decelerate,⁶ because they cannot overcome the force due to air resistance. ATP is the source of energy in all explosive sports, such as jumps, sprints, and weightlifting. Thus, if we produce a force with a nonvanishing velocity, that is, we produce mechanical power, the force is limited by the rate that our muscles can convert ATP into ADP.

To discuss the performance of a jumper, we use the results of two observations. One is the maximum force that athletes can produce in a small time interval with their legs while producing work. We will take this information from observations of the squat. In this exercise a weight is rested on the shoulders of an athlete. He starts from the upright position, and bends his ankles, knees, and hips as if sitting. At the lowest position, when his thighs are horizontal, he returns to the upright position. The maximum weight an athlete can lift doing a squat is about 5000 N. For a first class male athlete with mass 100 kg, the maximum force that can be made with just one leg is about 3000 N. (In the high and long jump, athlete's use just one leg to push their center of mass.) This force is different from a static force.

In both the high and long jump, the height of the runner's center of mass remains almost constant until the last stride. In the last stride the center of mass rises about 25 cm before the runner takes off and his foot loses contact with the ground.

From these two observations we conclude that an 80 kg runner (assuming 80 kg athlete can produce the same 3000 N force with each leg) can add about $(3000-800)\text{N} \times 0.25\text{ m} = 550\text{ J}$ to the kinetic energy. We will use this result in the following.

An equivalent result can be obtained from an analysis of an elite 100 m runner. At 6 m/s, an elite runner has an acceleration of about 5 m/s^2 (see, for instance, Fig. 1 in Ref. 6). For an 80 kg athlete this acceleration corresponds to a mechanical power of 2400 W. At every stride, the runner's center of mass rises about 5 cm. At a rate of 5 strides/s (a typical rate in the 100 m dash), the up-down movement of the center of mass corresponds to 200 W of additional power. Thus at each stride, the runner produces $(2400+200)\text{W} \times 0.2\text{ s} = 520\text{ J}$. If we also include a small contribution due to air resistance, this result is consistent with the previous estimate of 550 J.

For female runners, the time of the 100 m dash is about 10% greater, and the velocity about 10% smaller than the male records. Thus, we estimate that the acceleration and, hence the force, is about 20% smaller than that for male

Magnetostriction in an array of spin chains under a magnetic field

E. Orignac

Laboratoire de Physique Théorique de l'École Normale Supérieure, CNRS UMR8549, 24, Rue Lhomond, 75231 Paris Cedex 05, France

R. Citro

Dipartimento di Fisica "E. R. Caianiello" and Unità INFM di Salerno, Università degli Studi di Salerno, Via S. Allende, I-84081 Baronissi (Sa), Italy

(Received 18 October 2004; revised manuscript received 25 March 2005; published 23 June 2005)

We consider an array of XX spin-1/2 chains coupled to acoustic phonons and placed in a magnetic field. Treating the phonons in the mean field approximation, we show that this system presents a first-order transition as a function of the magnetic field between a partially magnetized distorted state and the fully polarized undistorted state at low temperature. This behavior results from the magnetostriction of the coupled chain system. A dip in the elastic constant of the material near the saturation field along with an anomaly in the magnetic susceptibility is predicted. We also predict the contraction of the material as the magnetic field is reduced (positive magnetostriction) and the reciprocal effect, i.e., a decrease of magnetization under applied pressure. At higher temperature, the first-order transition is replaced by a crossover. However, the anomalies in the susceptibilities in the system near the saturation field are still present. We discuss the relevance of our analysis in relation to recent experiments on spin-1/2 chain and ladder materials in high magnetic fields.

DOI: 10.1103/PhysRevB.71.214419

PACS number(s): 75.10.Pq, 75.10.Jm, 75.80.+q

I. INTRODUCTION

The subject of Bose-Einstein condensation (BEC) has become tremendously active both experimentally and theoretically in recent years due to the observation of BEC in trapped atomic gases.¹ Another way of obtaining a BEC, predicted theoretically some time ago is to place a quasi-one-dimensional spin gap system under a strong magnetic field²⁻⁹ causing the formation of a Luttinger liquid of magnons. This Luttinger liquid possesses a quasi-long-range order, which is a one-dimensional precursor of the BEC.¹⁰⁻¹² In the presence of any three-dimensional coupling, this quasicondensed state develops a long-range order, which corresponds to a BEC of the magnons.^{13,14} This condensation has been observed experimentally¹⁵ in spin-1 chain materials, and more recently¹⁶⁻¹⁸ in $\text{Cu}_2(\text{C}_5\text{H}_{12}\text{N}_2)_2\text{Cl}_4$ (CuHpCl), a material originally believed on the basis of its thermodynamics to be formed of weakly coupled two-leg ladders. However, it is now known that CuHpCl is in fact formed of dimers coupled in a three-dimensional network,¹⁹ and that the Bose condensation is a condensation of a two- or three-dimensional magnon Bose fluid.²⁰ Recently, such a Bose-Einstein condensation of magnons has also been observed in other coupled dimers systems such as TiCuCl_3 ,²¹ KCuCl_3 ,²² $\text{Cs}_3\text{Cr}_2\text{Br}_9$,²³ and $\text{BaCu}_2\text{Si}_2\text{O}_6$.²⁴ Theoretical description taking into account the two-dimensional nature of these gapped systems have been developed²⁵⁻²⁸ in recent years. They are based on the bond operator theory description of the coupled dimer system.²⁹⁻³¹ The interactions between the condensed triplet bosons are treated by the Hartree-Fock-Popov (HFP) approximation,³² and a rigid lattice is assumed. However, more recently, some experimental evidence for a lattice distortion associated with the Bose-Einstein condensation has been obtained.³³⁻³⁵ Older reports of specific heat anomalies also pointed to a lattice distortion associated with the

transition.³⁶ It has thus been suggested that the distortion observed in experiments could be the generalized spin-Peierls transition predicted originally for spin ladder systems under a field.³⁷ However, similarly to the conventional spin-Peierls transition,^{38,39} in a generalized spin-Peierls transition the lattice distortion results from an *optical* phonon becoming static. As a result, in the generalized spin-Peierls transition, the lattice constants of the crystal do not change, but superlattice peaks are visible in x-ray diffraction, in contrast with experiments.^{34,35} In fact, in the case of a condensate of magnetic excitations coupled to a deformable lattice, another instability than the generalized spin-Peierls transition is possible, namely, magnetostriction. Although magnetostriction has been mostly discussed in the context of ferromagnetism^{40,41} it can also be observed in paramagnetic or antiferromagnetic systems.⁴² In the case of magnetostriction, the lattice parameters change as the system becomes magnetized, but the number of atoms per unit cell does not change, which means that no new reflections appear in x-ray diffraction experiments.³⁵ In a ferromagnet, magnetostriction is known to turn the second-order Curie transition into a first-order transition.⁴³ Thus, the magnetostrictive effects may also explain the first-order transition as a function of magnetic field observed in magnon Bose-Einstein condensation experiments.³³⁻³⁵ Besides the Bose-Einstein condensation of magnons in spin gap systems, magnetostriction effects are also relevant near the saturation field in the spin-1/2 chain material $\text{Cu(II)-2,5bis(pyrazol-1-yl)-1,4-dihydroxybenzene}$ (CuCCP).⁴⁴ In fact, the two effects can be closely related as a ladder system under strong magnetic field can be mapped for strong rung coupling on an anisotropic spin-1/2 chain.⁴⁵ In the present paper, we will discuss a model of magnetostriction in one-dimensional (1D) XX spin chains coupled by 3D acoustic phonons. We will study the effect of phonon coupling at the mean field level and show that the Bose-Einstein condensation transition of the magnons becomes a

Schumann's resonances: A particular example of a spherical resonant cavity

M. F. Ciappina^{a)} and M. Febbo

Departamento de Física, Universidad Nacional del Sur, Av. Alem 1253, 8000, Bahía Blanca, Argentina

(Received 19 June 2003; accepted 9 January 2004)

The resonances between the Earth as one boundary and the ionosphere as the other, known as Schumann's resonances, represent an interesting example of a spherical cavity. We consider a simple model in which the boundaries behave as perfect conductors and then take into account the finite conductivity of the boundaries. Numerical results are obtained for both models and compared with available data. Good agreement is shown to exist between the analytical results and the experimental values when finite conductivity of the walls is considered. © 2004 American Association of Physics Teachers.

[DOI: 10.1119/1.1652037]

I. INTRODUCTION

If one thinks of a resonant cavity, the first thought that might come in mind is a microwave oven or a similar device. It might be difficult to believe that the Earth behaves like an enormous resonant cavity. This behavior was first realized by Nikola Tesla in the early 1900's. He thought that the Earth would be a conductor and be responsive to certain electromagnetic frequencies. The inner boundary of the cavity is provided by the Earth's surface while the ionosphere is the outer surface. The resonant frequencies of this cavity are known as *Schumann resonances* in honor of W. O. Schumann who predicted them in 1952¹ and detected them in 1954.²

To observe these electromagnetic waves, one has to excite the Earth resonant cavity near its resonance, which is what the electrical activity in the atmosphere does. The resonant waves manifest themselves as peaks in the electromagnetic noise spectrum and have average values of 8, 14, 20, 26, 32, 37, and 43 Hz, with a daily variation of about ± 0.5 Hz depending on the Earth's electromagnetic activity.³ Their characteristic wavelengths are of the order of magnitude of the Earth's radius (6400 km).

In this paper, we determine the Schumann resonances by considering two models. The first, a rather crude one, considers the cavity's walls as perfect conductors of infinite conductivity. The more realistic model takes into account the finite conductivity of the walls.

The paper is organized as follows. In Sec. II, the theoretical approach for perfectly conducting walls is developed. In Sec. III, we present two methods for obtaining the corrections for real conductive walls. One method includes the calculation of the quality factor Q . The other approach is based on the method of perturbation of boundary conditions.⁴ In Sec. IV, these methods are used to determine the improved eigenfrequencies of the system, and we compare these frequencies with the results for perfectly conducting walls and the available data. Concluding remarks are presented in Sec. V.

II. THEORY AND INFINITE CONDUCTIVITY APPROACH

Electric or magnetic fields in an electromagnetic cavity resonator can support different types of standing waves depending on the direction of their components. The directions

of the fields determine the characteristics of the electromagnetic modes inside a hollow spherical cavity. There are two types: transverse magnetic (TM) modes and transverse electric (TE) modes, depending on the existence of transverse magnetic or electric fields, respectively. In our problem, TM (TE) designates the non-existence of radial magnetic (electric) field component, that is, $B_r=0$ ($E_r=0$). We shall discuss only the TM modes because they present the lowest frequencies in comparison with TE modes for the Earth cavity.

We assume that the fields for a TM mode in our spherical cavity are independent of the azimuthal angle ϕ . From Maxwell's equation for zero divergence and the requirement that the fields must be finite at $\theta=0$, we conclude that only the ϕ component of \mathbf{B} is nonzero. Faraday's law requires that the ϕ component of the electric field \mathbf{E} also must vanish. Hence, the nonvanishing field's components for the TM mode are B_ϕ , E_r , and E_θ .

We first consider two perfectly conducting concentric spheres with inner radius R_i (the Earth's radius) and outer radius R_o , where $R_o=R_i+h$ and h is the height of the ionosphere. Although the ionosphere is the region of the atmosphere between 90 and 3000 km above the Earth's surface, the major electron density $10^8-10^{11} \text{ m}^{-3}$ is at about 50 km during the day and 300 km at night. It can be shown that for these values, the resonant frequencies vary only about ± 0.5 Hz for each mode. Therefore, we will assume $h=100$ km to compare with literature.⁵

We start with the vector Helmholtz equation⁴

$$\nabla^2 \mathbf{B} + \frac{\omega^2}{c^2} \mathbf{B} = 0, \quad (1)$$

which can be written in spherical coordinates as

$$\frac{\omega^2}{c^2} (rB_\phi) + \frac{\partial}{\partial r^2} (rB_\phi) + \frac{1}{r^2} \left[\frac{1}{\sin \theta} \frac{\partial}{\partial \theta} \left(\sin \theta \frac{\partial (rB_\phi)}{\partial \theta} \right) - \frac{(rB_\phi)}{\sin^2 \theta} \right] = 0. \quad (2)$$

To solve Eq. (2), we apply the method of separation of variables. We have

$$B_\phi(r, \theta) = \frac{f_l(r)}{r} g(\theta). \quad (3)$$

Osmium is not harder than diamond

B. R. Sahu and Leonard Kleinman

Department of Physics, University of Texas at Austin, Austin, Texas 78712-0264, USA

(Received 1 October 2004; revised manuscript received 27 June 2005; published 20 September 2005)

A recent measurement found Os has a larger bulk modulus than diamond, in agreement with an earlier calculation. We have made fully relativistic linear augmented plane-wave calculations of osmium and diamond and found diamond to have the larger bulk modulus, independent of whether the local-density- or generalized-gradient-approximation (GGA) exchange-correlation potentials are used. With the GGA our bulk modulus lies between two very recent and more accurate experimental values.

DOI: [10.1103/PhysRevB.72.113106](https://doi.org/10.1103/PhysRevB.72.113106)

PACS number(s): 71.20.Be, 62.20.Dc

Interest in the hardness of materials can be traced back at least as far as Galileo. Of the several definitions¹ of hardness, the theoretical hardness or bulk modulus is most amenable to measurement and calculation by physicists. Osmium is the most dense of all the elements, and diamond is the most atomically dense, which is consistent with diamond being the hardest element and Os the second hardest. Thus it is surprising that the first high-pressure bulk modulus measurement of Os was made only three years ago² and even more surprising that the first measurement found Os to have a bulk modulus considerably larger than the accepted experimental value for diamond. However, two very recent measurements^{3,4} found it to be more compressible. Takemura³ attributed the result of Cynn *et al.*² to their use of argon as a pressure transmitting medium, which is known to give large nonhydrostatic stresses above 9 GPa, while Occelli *et al.*⁴ also attributed it to their use of energy (rather than angle) dispersive x-ray diffraction. These results are all listed in Table I along with the result of several calculations including our own.

The calculational results are equally contradictory. Using the local density approximation (LDA) for exchange and correlation and the full potential linear muffin-tin orbital (FPLMTO) method, Fast *et al.*⁵ obtained $B=476.1$ GPa for Os which is even larger than the largest experimental value. They did not obtain a value for diamond with which to compare their Os result. Using the LDA and FPLMTO, Cynn *et al.*² obtained 444.8 GPa which is less than their experimental value. It is equal to the experimental value for diamond but less than their calculated value for diamond. Occelli *et al.*⁴ using both the LDA and generalized gradient approximation (GGA) in the PW91 form⁶ performed ultrasoft pseudopotential calculations. Their LDA (GGA) bulk modulus for Os was greater (less) than their experimental value but each was less than their calculated result for diamond with the corresponding exchange-correlation potential. Very recently Hebbache and Zemzemi⁷ using ordinary pseudopotentials found that the Os B_0 in any of the fitting formulas⁸⁻¹⁰ they used was larger (smaller) than that of diamond for small (large) pressure. They claimed that this meant Os was harder than diamond at low pressure. Since B_0 is the zero-pressure bulk modulus no matter what range of pressure is fit, what it actually means is that their high- and low-pressure calculations are inconsistent. Although Os is a hexagonal-close-packed (hcp) crystal, the only other calculation¹¹ of which we are aware was performed for face-centered-cubic (fcc) Os using

the LDA and ordinary pseudopotentials, in order to compare it with its carbide and nitride. None of these theoretical calculations included spin-orbit coupling which is important for heavy elements like Os. Moreover, the authors of Ref. 4 did not mention whether their calculation is done at a fixed c/a ratio for the set of volumes considered or if a full optimization of the c/a ratio was done. We perform fully relativistic full-potential all-electron calculations with both the LDA and GGA on hcp Os. Our calculated GGA bulk modulus value is very close to the experimental values of Refs. 3 and 4. To the best of our knowledge, this is the first theoretical work on hcp Os where all relativistic effects are taken into account for volume and c/a optimization. For comparison we also calculate the bulk modulus of carbon in the diamond structure and fcc Os.

To determine the structural properties of hcp Os and to determine whether it is harder than diamond or not we have performed fully relativistic full-potential linearized augmented plane-wave calculations.¹² The LDA (Ref. 6) and GGA (Ref. 13) were used as the exchange and correlation energy density functionals. A nonoverlapping muffin-tin (MT) sphere radius of 2.3 bohrs was used for the Os atom. The valence wave functions inside the MT spheres were expanded into spherical harmonics up to $l=10$ and the potential up to $l=6$. An APW+lo (Refs. 14 and 15) type basis set was used, and the Os $5s$ and $5p$ semicore states were treated as valence electrons. Integrals over the Brillouin zone (BZ) were performed with the quadratic tetrahedron method.¹⁶ Convergence of the total energy with respect to the plane-wave expansion parameter $R_{MT}K_{max}$ (where R_{MT} is the MT radius and K_{max} is the plane-wave cutoff) and the \mathbf{k} -point sampling was checked. Here 1183 (84) \mathbf{k} points in the full (irreducible wedge of) the hexagonal BZ and $R_{MT}K_{max}=8$ turn out to be sufficient for accuracy of the calculated total energy (0.01 mRy/unit cell). For each unit cell volume, we optimized the c/a ratio. For fcc Os 1687 (120) \mathbf{k} points were used in the full (irreducible) BZ and for diamond 729 and 35 \mathbf{k} points were used.

After the initial equilibrium volume¹⁷ was determined the energy was calculated for volumes differing by $\pm 2n\%$ ($1 \leq n \leq 6$). For Os we display results in Table II using all calculated volumes between $\pm 8\%$, $\pm 10\%$, and $\pm 12\%$ for three different equation of states (EOS) fitting formulas.⁸⁻¹⁰ For very small volume changes the change in energy is small

Abstract Submitted
for the MAR05 Meeting of
The American Physical Society

Sorting Category: 06.11.5 (E)

Time-resolved Spin Dynamics in Semiconductor Microdisk Lasers¹ SAYANTANI GHOSH, YONGQING LI, FLORIAN MEIER, ROBERTO MYERS, DAVID D. AWSCHALOM, Center for Spintronics and Quantum Computation, University of California, Santa Barbara, CA 93106, WEI-HUA WANG, NITIN SAMARTH, Department of Physics, Penn State University, University Park PA 16802 — Optical microcavities offer unique means of controlling the interaction of light and matter, which have led to the development of a wide range of applications in optical communications and have stimulated discussions of quantum computational schemes based on cavity QED. We present a study of the dynamics of optically injected spins in GaAs/AlGaAs multiple quantum well microdisk lasers, where emission intensity and line width measurements reveal very high quality factor modes, using a pump-probe, time-resolved Kerr rotation technique with picosecond resolution. We measure the spin decoherence as a function of the pump wavelength and input power and find that the spins in these structures couple selectively to the cavity modes at the resonant wavelengths. This is manifested by an enhancement of the spin decoherence time at the lasing threshold of the cavity modes followed by a sharp decrease at greater pump power, where the stimulated emission dominates the radiative decay.

¹Work supported by DARPA QUIST

Prefer Oral Session
 Prefer Poster Session

Sayantani Ghosh
sghosh@iquest.ucsb.edu
Center for Spintronics and Quantum Computation
University of California, Santa Barbara, CA 93106

Date submitted: 22 Nov 2004

Electronic form version 1.4

Abstract Submitted
for the MAR05 Meeting of
The American Physical Society

Sorting Category: 17.5 (C)

Auxiliary Field Quantum Monte Carlo Study of Ground State Properties of Atoms and Molecules¹ MALLIGA SUEWATTANA, College of William and Mary, SHIWEI ZHANG, College of William and Mary, HENRY KRAKAUER, College of William and Mary, ERIC WALTER, College of William and Mary — We apply a recently developed quantum Monte Carlo (QMC) method ² to calculate the ground state properties of several atoms and molecules. The QMC method projects the many-body ground state from a trial state by random walks in the space of Slater determinants. The Hubbard-Stratonovich transformation is employed to decouple the Coulomb interaction between electrons. A trial wave function $|\Psi_T\rangle$ is used in the approximation to control the phase problem in QMC. We also carry out Hartree-Fock (HF) and density functional theory (with the local density approximation (LDA)) calculations. The generated single Slater determinant wave functions are used as $|\Psi_T\rangle$ in QMC. The dissociation and ionization energies are calculated for Aluminum, Silicon, Phosphorous, Sulfur, Chlorine and Arsenic atoms and molecules. The results are in good agreement with experimental values.

¹Supported by NSF and ONR

²Shiwei Zhang, Henry Krakauer, Phys. Rev. Lett. **90**. 136401 (2003).

Prefer Oral Session
 Prefer Poster Session

Malliga Suewattana
cherry@camelot.physics.wm.edu
College of William and Mary

Date submitted: 01 Dec 2004

Electronic form version 1.4

SIZE-DEPENDENT ELECTRON-IMPACT DETACHMENT OF INTERNALLY COLD NEGATIVE CLUSTERS

M. Erritt,^{1,2} A. Diner,¹ Y. Toker,¹ O. Aviv,¹ D. Strasser,¹ O. Heber,¹ I. Ben-Itzhak,^{1,3} A. Wolf,⁴ D. Schwalm,⁴ M. L. Rappaport¹ and D. Zajfman^{1,4}

1) Department of Particle Physics, Weizmann Institute of Science, Rehovot, 76100, Israel

2) Inst. f. Physik, University of Greifswald, D-17487 Germany

3) J.R. Macdonald Laboratory, Kansas State University, Manhattan, Kansas 66506 USA

4) Max-Planck-Institut für Kernphysik, D-69117 Heidelberg, Germany

Electron-impact detachment is a process that has been extensively studied for atoms and small molecules. It has been shown that for such simple species, the electron binding energy E_b is the most important parameter in the determination of both the threshold behavior and the magnitude of the cross section above threshold. A simple scaling law has been obtained [1].

$$(1) \quad \sigma \propto \left[\frac{1}{E_b} \right]^2$$

It was shown in previous publication that the scaling law does not hold even for small carbon clusters [2].

Here we report about a systematic study of the cross sections for electron detachment of internally cold C_n^- , Al_n^- and Ag_n^- . The clusters were produced in a Cs sputter source and injected into an electrostatic ion trap fitted with an internal electron target. The injected clusters were relaxed to their ground electronic and vibrational state in few hundreds of milliseconds and were then crossed by an electron beam with relative collision energy between 5-50 eV [3].

Figure 1 shows the electron-impact detachment cross sections for the C_n^- ($n = 1-12$) clusters at electron impact energy of 20 eV, normalized to the known cross section of C_2^- from Ref. 1. It is clearly seen that the cross section exhibits an even-odd oscillations reflecting the binding energy trend, namely, higher cross sections for weaker binding energies. It also indicates a change between linear chains ($n=2-9$) and rings ($n=10-12$). Surprisingly, however, these cross sections increase on the

average with cluster size, n , in spite of the increase in electron binding as expected from Equation 1 and shown by the solid line in Figure 1. In contrast, Al_n^- ($n = 2-5$) clusters follow the known scaling laws for electron detachment. We suggest that the size-dependent polarizability of these clusters is responsible for the observed behavior [2]. Additional data of metallic clusters of Ag^- will also be presented.

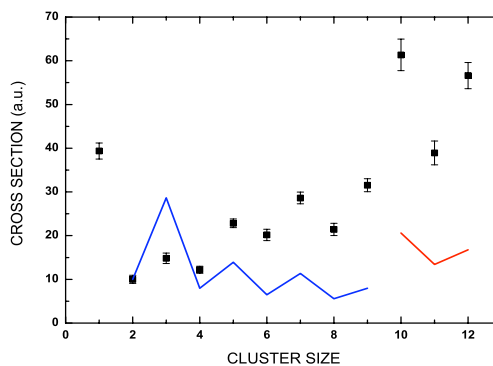


Figure 1: Electron impact detachment of carbon cluster. The points are the measured data while the lines were calculated from Eq. (1).

References

- [1] L.Vejby-Christensen et al., Phys. Rev. A 53, 2371 (1996).
- [2] A. Diner et al., Phys. Rev. Lett. 93, 063402/1-4 (2004).
- [3] O. Heber et al., Rev. Scientific Instr. 76, 013104 (2005).